

Microstructural Development and Mechanical Properties of Interrupted Aged Al-Mg-Si-Cu Alloy

J. BUHA, R.N. LUMLEY, and A.G. CROSKY

The effects of a recently developed interrupted aging procedure on the microstructural development and mechanical properties of the commercial Al-Mg-Si-Cu alloy 6061 have been studied using transmission electron microscopy (TEM), differential scanning calorimetry (DSC), and mechanical testing. This so-called T6I6 temper involves partially aging the alloy at a typical T6 temperature (the underaging stage), quenching, then holding at a reduced temperature (in this case 65 °C) to facilitate further hardening (the secondary aging stage), prior to final aging to peak properties at, or close to, the initial aging (T6) temperature (the reaging stage). The T6I6 aging treatment produces simultaneous increases in tensile properties, hardness, and toughness, as compared with conventional T6. The overall improvement in the mechanical properties of 6061 T6I6 is associated with the formation of a greater number of finer, and more densely dispersed, β'' precipitates in the final microstructure. Secondary precipitation took place during the interrupted aging stage of the T6I6 temper, resulting in the formation of a large number of Guinier-Preston (GP) zones that served as precursors to the needlelike β'' precipitates when elevated temperature aging was resumed.

I. INTRODUCTION

MOST heat-treatable aluminum alloys are commonly subjected to a single stage, T6 aging treatment following solution heat treatment and quenching. Two types of modified heat treatments have been developed, termed “T6IX” wherein artificial aging at a typical T6 aging temperature is interrupted (I) by holding the alloy at a reduced temperature for a prolonged period of time.^[1–5] In the first of these heat treatments, aging is allowed to continue at the reduced temperature, hence the designation T6I4 (*cf.* T4) and typically produces tensile properties close to, or sometimes greater than, those for the T6 temper.^[3,4] If artificial aging is resumed after the interrupt, a wide range of aluminum alloys show a simultaneous improvement in both the tensile and fracture properties, compared to the T6 condition.^[1,2,3] This heat treatment has been designated a T6I6 temper. The process of secondary precipitation during the interrupted aging stage is responsible for the improvements observed.^[2,3]

For many years, it has been widely assumed that once an aluminum alloy is artificially aged at an elevated temperature (*e.g.*, a T6 temper), its microstructure and mechanical properties remain stable for an indefinite time if the alloy is then exposed to a significantly lower temperature. However, Löffler *et al.*,^[6,7] reported that highly saturated Al-Zn alloys, aged initially at 180 °C, were found to undergo what has been termed “secondary precipitation” if the alloy was then held at ambient temperature. Secondary precipitation is observed when underaged, and sometimes even fully aged alloys, are held at a reduced temperature for an

extended period of time. As a result, the mechanical properties of the material are altered. For example, in the Li-containing aluminum alloy 2090, secondary aging of peak-aged material has been found to reduce ductility and fracture toughness, and this has been ascribed to secondary precipitation of a fine dispersion of the Al_3Li (δ') hardening phase throughout the matrix.^[8] Secondary precipitation was also found to reduce the positive creep performance in the underaged condition of an experimental Al-Cu-Mg-Ag alloy.^[9] Because secondary precipitation in aluminum alloys occurred generally in an uncontrolled manner, and in such cases had mostly an adverse effect on the mechanical properties, this phenomenon was initially considered to be problematic and undesirable. However, it has been shown recently that through the T6I6 aging procedure, secondary precipitation can also be manipulated and exploited to enhance the mechanical properties of a wide range of age-hardenable aluminum alloys.^[1–5,10]

Alloys based on the Al-Mg-Si-Cu system are widely used as medium strength alloys with major applications in extruded products and automotive body sheet. AA6061 is one of the most widely used alloys from this group and optimal mechanical properties are achieved by aging in the temperature range from 175 °C to 180 °C for 10 to 20 hours after solution treatment and quenching (T6 temper). These alloys undergo a complex decomposition during heat treatment and, for compositions with a balanced Mg to Si ratio, the precipitation sequence is now widely accepted as being^[11–15]

SSSS \rightarrow clusters/co-clusters of Mg and

Si \rightarrow GP zones $\rightarrow \beta'' \rightarrow \beta'$; $Q' \rightarrow \beta(\text{Mg}_2\text{Si}); Q$

The initial stages of precipitation and the formation of needle-shaped β'' phase are of greatest importance for the commercial heat treatment of Al-Mg-Si-Cu alloys. Clustering and coclustering of Mg and Si atoms have been observed in naturally aged and low-temperature aged alloys.^[12,16,17] The needlelike β'' precipitate, which evolves from the fully

J. BUHA, formerly Postgraduate Student, School of Materials Science and Engineering, University of New South Wales, is JSPS Fellow, National Institute for Materials Science, Tsukuba, 305-0047 Ibaraki, Japan. Contact e-mail: buha.joka@nims.go.jp R.N. LUMLEY, Research Scientist, is with Manufacturing and Infrastructure Technology, Commonwealth Scientific and Industrial Research Organisation (CSIRO), Clayton South MDC, VIC 3169, Australia. A.G. CROSKY, Professor, is with the School of Materials Science and Engineering, University of New South Wales, Sydney, NSW 2052, Australia.

Manuscript submitted December 23, 2005.

coherent GP zones, is considered to be the most effective strengthening phase in these alloys.^[18,19,20] Rodlike β' and a Cu-bearing lath-shaped Q' phase, as well as the corresponding equilibrium β and Q phases, are precipitates that form in highly overaged alloys. These precipitates produce only limited strengthening and are not characteristic of the peak-aged T6 condition.^[12,14,15,21,22]

The objective of the present work was to determine the effects of the T6I6 interrupted aging heat treatments on the precipitation process, microstructural development, and mechanical properties of alloy 6061. Special attention was given to the study of secondary precipitation using transmission electron microscopy (TEM) and differential scanning calorimetry (DSC).

II. EXPERIMENTAL METHODS

Alloy AA6061 was provided in the form of a homogenized extrusion billet. The composition, which is given in Table I, is balanced with respect to the content of Mg and Si (*i.e.*, Mg:Si at. pct \approx 2). Sections $\sim 120 \times 70 \times 20$ mm (L \times B \times W) were cut from the starting material for further processing. All specimens were solution treated at 560 °C for 2 hours in a circulating air furnace, followed by cold water quenching. A number of different artificial aging treatments were examined and these are shown schematically in Figure 1. Specific details of these heat treatments are given in Table II. In the first condition, the as-solution-treated and quenched alloy was subjected to the conventional T6 heat treatment (dashed line in Figure 1) by aging at 177 °C. The alloy was also subjected to a number of different T6I4 aging treatments, which involved underaging at 177 °C for times between 10 minutes and 6 hours, followed by quenching, and then secondary aging at 65 °C. For the T6I6 treatments, after 20 minutes of artificial aging at 177 °C, the heat treatment was interrupted by quenching. The alloy was then held at 65 °C for a period of 2 weeks to facilitate further hardening (secondary aging). Finally, the alloy was reheated and held at either 177 °C or 150 °C (hereafter termed "T6I6/177" and "T6I6/150," respectively) to complete the interrupted aging cycle. Additionally, the as-quenched alloy was aged for 2 weeks at either room temperature (RT) or 65 °C prior to artificial aging at 177 °C in order to examine the effect of low-temperature preaging on the development of microstructure at 177 °C. All artificial aging at 177 °C was performed in an oil bath followed by quenching in petroleum ether. Aging at 65 °C was performed in a circulating air furnace, followed by water cooling.

Vickers hardness measurements, made with a 10-kg load, were used to monitor hardness changes during all aging treatments. The hardness data reported here represent the average of at least three measurements. Tensile and fracture properties were determined for material in the T6, T6I6/177, and T6I6/150 peak-aged conditions. For each different

peak-aged condition, five tensile samples and three fracture toughness/damage tolerance* samples were cut from the

*Plane strain fracture conditions are not possible for alloy 6061 and therefore the term "damage tolerance" will be used throughout.

heat-treated sections. The tensile properties were determined in the longitudinal direction in accordance with Australian Standard AS 1391 to 1991. The samples had a gage length of 25 mm, a gage width of 4 mm, and a gage thickness of 4 mm. The damage tolerance was determined in the S-L orientation using the chevron notch procedure given in ASTM E1304-97.

Conventional transmission electron microscopy (TEM), both bright field (BF TEM) and dark field (DF TEM), as well as high-resolution TEM (HRTEM), was used to study the development of microstructure during the aging treatments. The specimens for all the TEM observations were taken from sections perpendicular to the longitudinal direction and were prepared using standard specimen preparation techniques and electropolished in a solution of 30 pct nitric acid in methanol. The thin foils were examined in a PHILIPS** CM200 TEM operated at 200 kV. The median

**PHILIPS is a trademark of Philips Electronic Instruments Corp., Mahwah, NJ.

length of the elongated precipitates (β'') in the peak-aged condition was determined for each of the tempers examined. The results reported here were determined with a level of statistical confidence equal to, or higher than, 90 pct with a ± 7 pct error interval on the data set. The precipitate length was measured from TEM images in the $[001]_{Al}$ orientation, using AnalySIS software and at least 5 images. These were taken at the same magnification from different

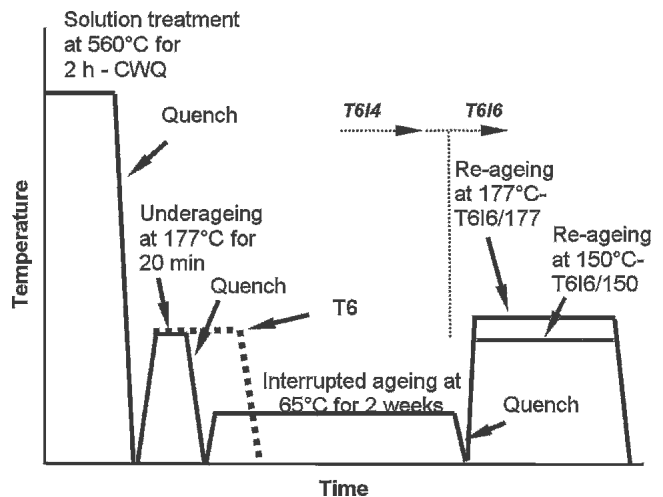


Fig. 1—Schematic diagram showing the T6, T6I6/177, and T6I6/150 heat treatments.

Table I. Chemical Composition (Weight Percent) of the AA6061 Alloy Examined

Alloy	Si	Mg	Cu	Fe	Cr	Zn	Mn	Ti
AA6061	0.59	0.99	0.25	0.16	0.112	0.002	0.13	0.012

Table II. Description of Heat Treatments Examined

Number	Heat Treatment	Description and Aging Times			
1	T6	Aging at 177 °C for 4, 15, and 160 h			
2	T6I4	Solution treatment at 560 °C for 2 h-cold water quench	Quenching	Secondary aging at 65 °C for up to 385 h	
3	T6I6/177			Secondary aging at 65 °C for 2 weeks	Reaging at 177 °C for 6, 15, and 160 h
4	T6I6/150				Reaging at 150 °C for 6, 15, and 160 h
5	65 °C/2 w-177 °C			Preaging at 65 °C for 2 weeks	Aging at 177 °C for up to 120 h
6	RT/2 w-177 °C			Preaging at room temperature for 2 weeks	

areas for each of the conditions examined. In the [001]_{Al} orientation, precipitate particles measured were viewed edge on.

Differential scanning calorimetry (DSC) was carried out in a TA Instruments (New Castle, DE) 2010 cell with high-purity aluminum used as a reference. The heating rate used was 10 °C/min. A baseline thermogram was recorded from the pure Al reference sample and subsequently subtracted from the alloy thermograms. The weight of the specimens was 100 ± 5 mg. Each DSC scan was repeated at least 3 times to confirm the reproducibility of the results.

III. RESULTS

A. Mechanical Properties

Figure 2 shows the hardness curve for 6061 in the T6 condition, as well as the response of the alloy to secondary aging at 65 °C following aging at 177 °C for times between 10 minutes and 6 hours. For the T6 heat treatment, the hardness increased rapidly during the first hour of aging and there was then little change for about 50 hours until softening occurred as the alloy overaged. A peak hardness of 134 VHN was reached after about 15 to 18 hours. The secondary hardening curves in Figure 2 show that the underaged 6061 had a significant response to secondary aging at 65 °C for all of the conditions examined. The greatest increment in hardness from the secondary aging treatment was obtained for the specimens aged for the shortest times (10 and 20 minutes). For this reason, underaging at 177 °C for 20 minutes and then secondary aging at 65 °C for 2 weeks was used as the precursor to the reaging stage for both the T6I6/177 and T6I6/150 tempers.

The aging curves for the T6I6/177 and T6I6/150 tempers are compared to the T6 curve in Figures 3(a) and (b). The initial 20 minutes of underaging induced substantial hardening (~80 pct of the T6 peak hardness), with the hardness being further increased to nearly 90 pct of the T6 peak hardness after the interrupt stage at 65 °C. The reaging

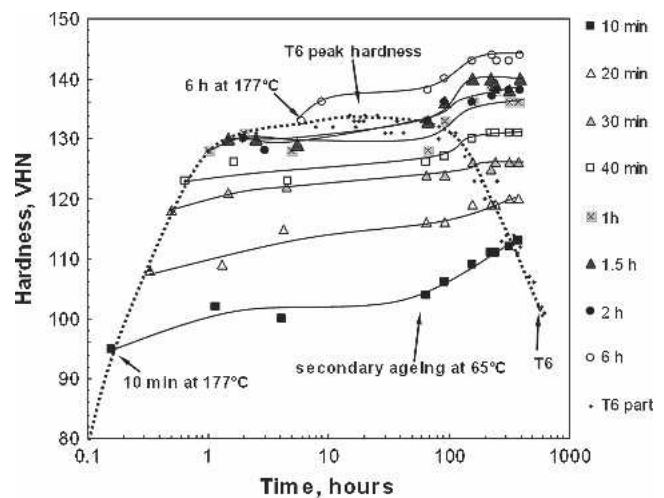


Fig. 2—Comparison of the T6 hardness curve (solid diamonds and dashed line) with the T6I4 aging curves for secondary aging at 65 °C (solid lines) following underaging at 177 °C for times between 10 min and 6 hours, as indicated in the graph.

stages of both the T6I6/150 and T6I6/177 tempers induced further hardening with the peak hardness values being 142 and 146 VHN, respectively, exceeding the T6 values by 6 and 9 pct.

Table III provides a comparison of the tensile properties and the damage tolerance for the three tempers examined. It can be seen that both T6I6 heat treatments produce improvements in the ultimate tensile strength (UTS). This was accompanied by a substantial increase in the damage tolerance, particularly for the T6I6/150 temper (36 pct increase for the T6I6/150, 21 pct increase for T6I6/177). An improvement of approximately 8 pct in the 0.2 pct proof stress was also achieved through the T6I6/177 heat treatment without significant change to the ductility of the alloy, whereas the 0.2 pct proof stress of the T6I6/150 temper was slightly lower than for the T6 alloy.

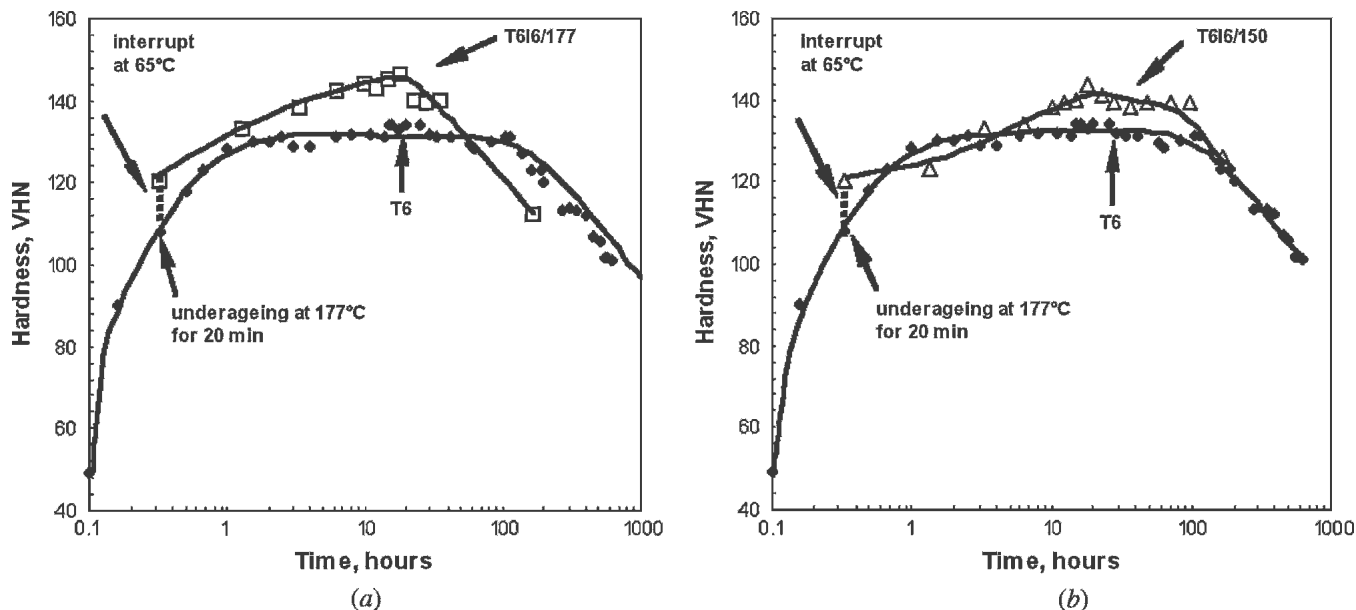


Fig. 3—Comparison of T6 (solid diamonds) and T6I6 hardness curves: (a) T6I6/177 (open squares) and (b) T6I6/150 (open triangles). The dashed line indicates hardness increment during secondary aging at 65 °C for 2 weeks.

Table III. Tensile Properties and Damage Tolerance of 6061 in T6 and T6I6 Peak-Aged Conditions

Temper	0.2 Pct			
	Proof Stress, MPa	UTS, MPa	Elongation, Pct	Damage Tolerance K_{qvm} , $MPa\sqrt{m}$
T6	311	352	8.2	30.5
T6I6/177	335	368	7.3	37
T6I6/150	302	369	11.6	41.6

B. Development of Microstructure

1. T6, T6I6/177, and T6I6/150 microstructures

In order to examine the correlation between the measured mechanical properties and the microstructure, representative specimens from the T6, T6I6/177, and T6I6/150 tempers were examined using TEM. Figures 4(a) through (i) illustrate the development of microstructure during the T6, T6I6/177, and T6I6/150 heat treatments in the underaged, peak-aged, and overaged conditions.

Figures 4(a) through (c) show BF TEM images obtained from material subjected to the conventional T6 heat treatment. After 4 hours of aging (Figure 4(a)), regions of dark contrast up to 5 nm in diameter can be seen, caused by elastic strain induced by fine coherent precipitates. Indeed, the HRTEM image of one of these precipitates (inset image in the upper left corner of Figure 4(a)) shows that the morphology is spheroidal and that aluminum {200} planes run continuously through the region of the precipitate, confirming they are fully coherent. These precipitates were therefore identified as GP zones.^[12,16] A few very fine elongated precipitates aligned along $\langle 001 \rangle_{Al}$ directions (arrowed), which appeared to be the β'' phase, were also observed. The morphology of the precipitates in this microstructure, as well as the presence of faint diffuse streaking

(arrowed) in the selected area electron diffraction (SAED) pattern, suggested the presence of both GP zones and β'' phase at this stage of aging. Figure 4(b) shows the peak-aged condition in which needlelike β'' precipitates, 15- to 60-nm long, aligned with $\langle 001 \rangle_{Al}$ directions, are observed. These precipitates coarsened with further aging and gradually transformed into β' precipitates, as seen after 160 hours of aging at 177 °C (Figure 4(c)). It is likely that some of the precipitates that appeared lath shaped in cross section were the Q' precipitates, commonly observed in the overaged condition of alloys containing Cu.^[13–15,22]

Figures 4(d) through (f) show the underaged, peak-aged, and overaged T6I6/177 microstructures, respectively. A high density of fine GP zones was observed following 6 hours of reaging at 177 °C and a small number of well-defined β'' needles (arrowed) was also seen (Figure 4(d)). Very fine β'' precipitates, approximately 5- to 40-nm long, were observed in the peak-aged microstructure after 15 hours of reaging (Figure 4(e)). These precipitates were very densely and evenly distributed. Some precipitates displaying the characteristics of GP zones were also clearly present. Further aging caused coarsening of these precipitates and the formation of β' rods and Q' laths (Figure 4(f)).

Figures 4(g) through (i) show that the T6I6/150 aging treatment resulted in an even higher level of refinement of the precipitates in the microstructure than the T6I6/177 treatment. A very high density of extremely fine precipitates, most likely GP zones, was observed after 6 hours of reaging at 150 °C (Figure 4(g)). After 15 hours of reaging, fine needles of the β'' phase were observed in the BF images and characteristic streaking in the SAED pattern was noted (arrowed in Figure 4(h)). The β'' precipitates were less than 10 nm in length, with occasional needles being up to 20 nm in length. However, a significant number of the fine precipitates present in the peak-aged microstructure

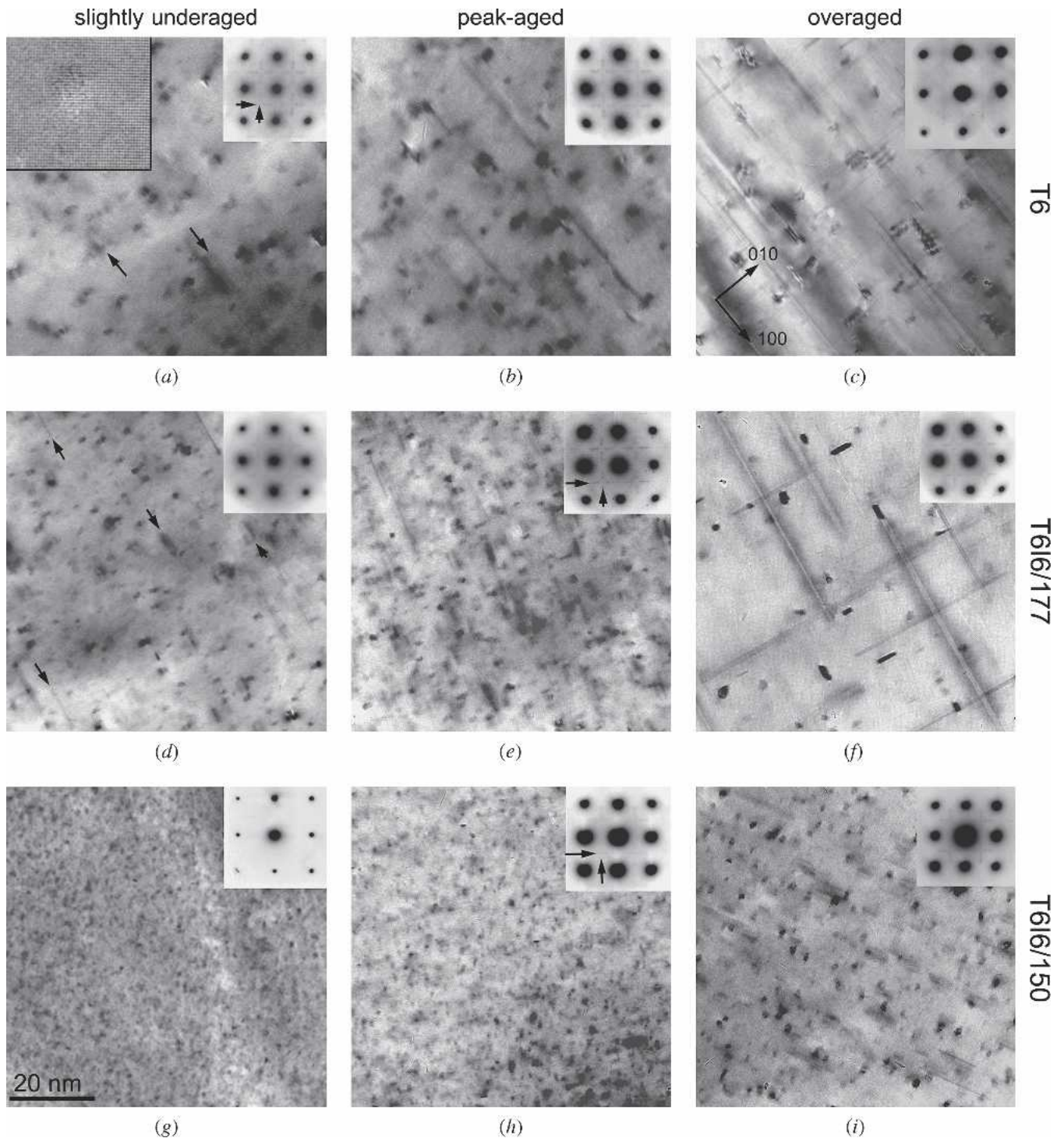


Fig. 4—BF TEM images taken with an $\langle 001 \rangle_{Al}$ orientation showing the following: (a) through (c) T6 microstructures aged for 4, 15, and 160 h, respectively; (d) through (f) T6I6/177 microstructures after reaging at 177 °C for 6, 15, and 160 h, respectively, following 20-min underaging at 177 °C and 2-week secondary aging at 65 °C; and (g) through (i) T6I6/150 microstructures after reaging at 150 °C for 6, 15, and 160 h, respectively, following 20-min underaging at 177 °C and 2-week secondary aging at 65 °C. All images were taken at the same magnification. Inset images in the top right corner show corresponding $\langle 001 \rangle_{Al}$ SAED patterns. Inset image in the top left corner in image (a) is a HRTEM image. The SAED patterns do not indicate the orientation of precipitates in the BF images.

appeared to be fully coherent GP zones. The lower reaging temperature also reduced the kinetics of transformation so that, even after 160 hours of reaging at 150 °C, the β'' precipitates remained the dominant phase in the microstructure (Figure 4(i)).

2. Secondary precipitation during interrupted aging

Figures 3 and 4, together with the results presented in Table III, indicate that insertion of an interrupted aging stage at 65 °C into a typical T6 heat treatment for AA6061 promotes the formation of a high density of

precipitates in the final microstructure that improves the mechanical properties. The development of the microstructure during the underaging and interrupted aging stages of the T6I6 heat treatments was therefore examined by TEM. Figure 5 shows BF TEM images from material (a) as-solution-treated and quenched, (b) underaged at 177 °C for 20 minutes, and (c) after subsequent interrupted aging at 65 °C for 2 weeks. The specimens were stored in liquid nitrogen between quenching and electropolishing and between electropolishing and examination in the microscope for all conditions examined (electropolishing was performed at ~ -45 °C). Any exposure at RT was kept to less than 30 seconds.

Figure 5(b) shows contrast arising from very fine and fully coherent precipitates, identified in earlier work as GP zones,^[12,16] in the material underaged at 177 °C for 20 minutes. This is in contrast to the microstructure of the as-solution-treated and quenched sample shown in Figure 5(a), where no evidence of precipitation can be seen. Figure 5(c) shows a much higher concentration of fine precipitates characteristic of GP zones that formed during the 65 °C dwell period. The SAED pattern from this specimen did not show any evidence of diffuse streaking that would indicate the presence of β'' precipitates. This implies that the precipitates formed during secondary aging are indeed GP zones. This is consistent with the hardness measurements and suggests that a considerable amount of solute remained in solid solution after the 20-minute underaging at 177 °C, which subsequently underwent secondary precipitation during the 2 weeks of interrupted aging at 65 °C. This resulted in the observed hardness increase of 12 VHN. Since GP zones are known to be the precursors to the major strengthening phase, β'' , the increase in the density of GP zones during interrupted aging would be expected to facilitate an increased density of the β'' precipitates during the reaging stage of the T6I6 heat treatments.

C. Comparison of Peak-Aged Microstructures

The BF TEM observations presented in Figure 4 confirm that interrupted aging promotes formation of a higher den-

sity of finer precipitates in the final microstructures of the T6I6 tempers compared to the T6 microstructure. The TEM observations also indicate that the dominant phase in each of the three peak-aged tempers was β'' . This phase is known to be the most effective strengthening precipitate in 6xxx series alloys,^[18,19,20] and any modification in the number and size of these precipitates would directly affect the mechanical properties of the alloy. However, the peak-aged microstructures, especially in the T6I6 peak-aged tempers, also contained a considerable number of GP zones. Further observations were therefore conducted by means of dark-field TEM imaging in order to determine if the T6I6 aging procedure led to an increase in the density of β'' precipitates as part of the overall increase in the density of the precipitates. In addition, the effect of interrupted aging on the length of the β'' precipitates was determined from measurements performed on the BF TEM images.

The DF TEM images, shown in Figures 6(a) through (c), were obtained from the $\langle 001 \rangle_{Al}$ zone axis so that the objective aperture was centered on a forbidden 110 matrix reflection, thereby selecting the diffuse streaking caused by the β'' precipitates aligned parallel with the electron beam.^[23] As a result, the DF images revealed only β'' needles viewed end-on (*i.e.*, only one-third of the total number of β'' precipitates). It is apparent from Figure 6 that the density of β'' needles was greater in both of the T6I6 tempers than in the T6 temper. The increase in density of the β'' phase observed in the T6I6/177 tempers correlates with the improvement in the mechanical properties of this temper. In the case of the T6I6/150 temper, the DF TEM image indicated an increase in the density of the fine β'' precipitates, and it will be recalled that the corresponding BF TEM image (Figure 4(h)) showed that these precipitates were significantly smaller in size than in either the T6 or the T6I6/177 temper.

Figure 7 shows the distribution of lengths of the β'' precipitates in the peak-aged T6, T6I6/177, and T6I6/150 microstructures (it was assumed that all elongated precipitates were β''). The bar chart given in Figure 7(a) shows that for the peak-aged T6 temper, the length of the β'' precipitates ranged from approximately 15 to 70 nm, with

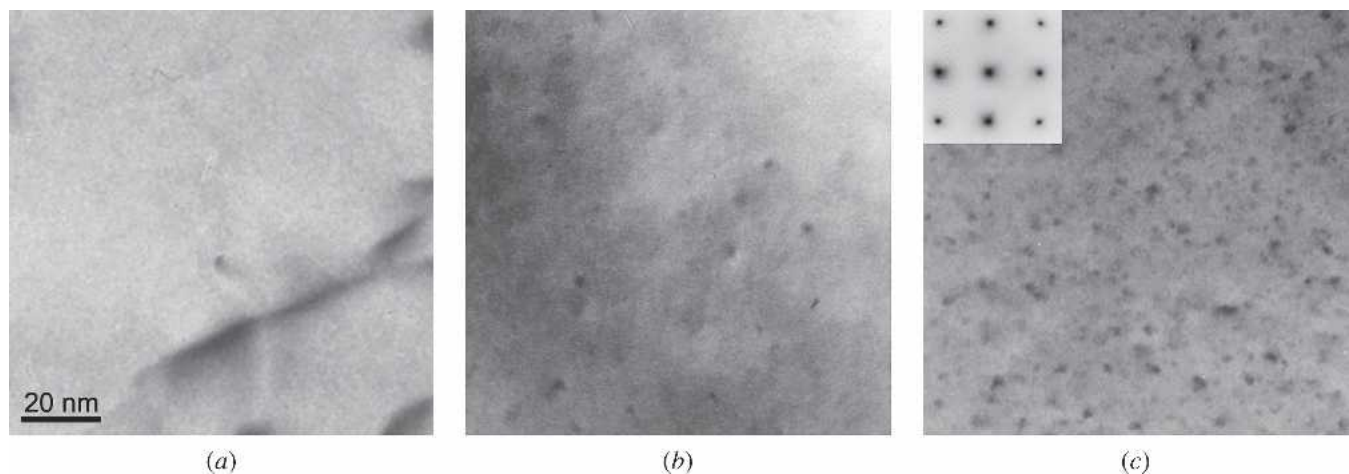


Fig. 5—BF TEM images showing the development of microstructure during underaging and secondary aging: (a) as solution treated and quenched, (b) after 20 min of aging at 177 °C, and (c) after 20 min at 177 °C and 2 weeks at 65 °C; the inset image shows the corresponding $\langle 001 \rangle_{Al}$ SAED pattern. All images were taken at the same magnification.

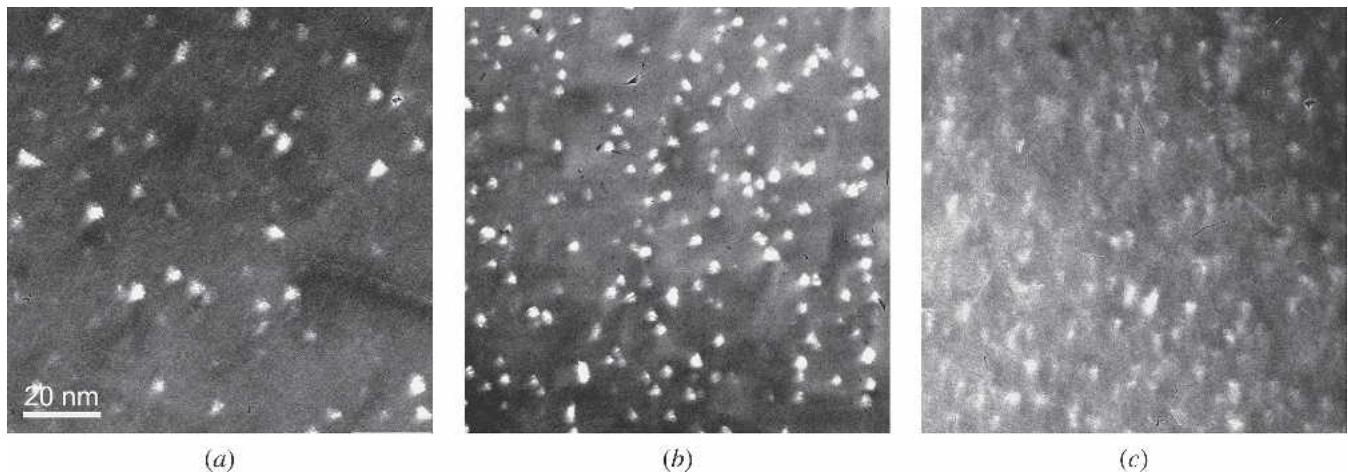


Fig. 6—Comparison of (a) T6, (b) T6I6/177, and (c) T6I6/150 peak-aged microstructures. DF TEM images taken with $\langle 001 \rangle$ matrix orientation showing the β'' precipitates parallel with the electron beam (bright spots). All images were taken at the same magnification.

65 pct of the precipitates being within the 30- to 45-nm range and the percentages on either side of this range being approximately equal. The median length of the β'' needles was 35 nm. For the T6I6/177 temper (Figure 7(b)), the length of the β'' precipitates ranged between about 7.5 and 60 nm, with about 65 pct of these precipitates now being between 10- and 15-nm long. Precipitates longer than 15 nm were present in a considerably greater number than those shorter than 10 nm, and the median length of precipitates in this temper was 12 nm. For the T6I6/150 peak-aged condition, the very high density and very small size of all the precipitates made distinction between the β'' precipitates and the GP zones difficult. However, those precipitates that could be identified as being elongated, and could also be measured from the images, were 5- to 20-nm long with more than 55 pct of these precipitates being approximately 7.5 nm. The median length of the elongated precipitates in this temper was 7 nm (Figure 7(c)).

D. Low-Temperature Preaging Prior to Artificial Aging

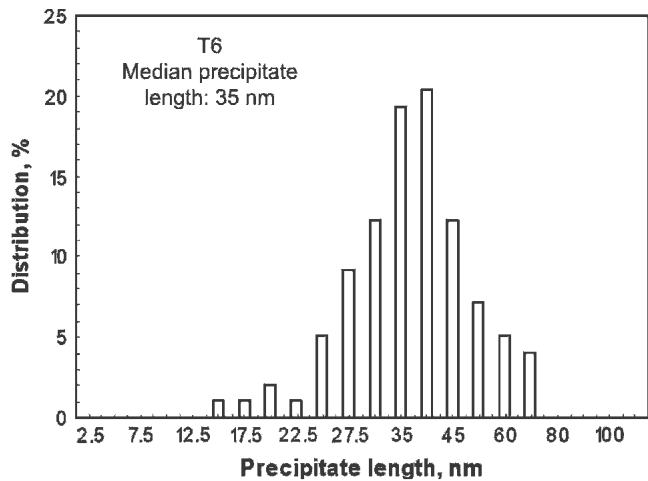
The TEM observations presented in Figure 5 suggest that both the underaging and interrupted aging stages of the T6I6 heat treatment led to precipitation of GP zones. Accordingly, a study was made to see if a simpler procedure, such as preaging at a reduced temperature prior to artificial aging, would also benefit the microstructural development and mechanical properties of 6061. Both aging at 25 °C and aging at 65 °C prior to artificial aging at 177 °C were conducted.

Figure 8(a) shows the hardness measurements made from a specimen aged for 2 weeks at 65 °C, following solution treatment and quenching, and then aged at 177 °C until overaged. The peak hardness was reached after 30 hours of aging, and, although a moderate increase in hardness above the T6 condition was observed, the corresponding micrograph from the peak-aged condition given in Figure 9(a) showed very coarse and widely spaced β'' precipitates having a median length of 48.5 nm (Figure 10(a)). This dispersion was coarser than was observed for the T6 and T6I6 tempers at peak hardness (Figures 4 and 7). Figure 8(b) shows the hardness measurements made on a specimen

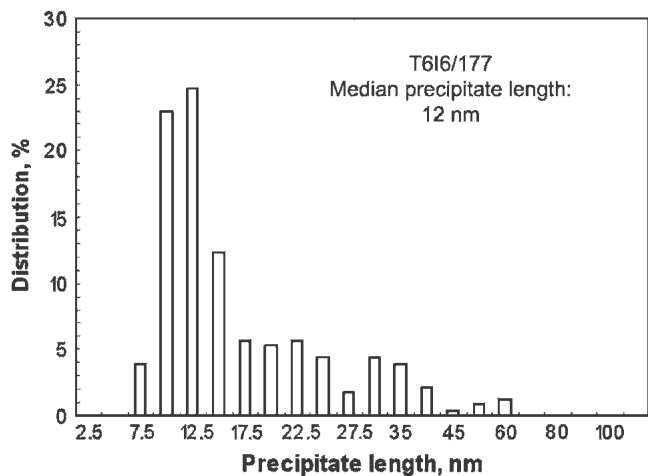
naturally aged at 25 °C for 2 weeks prior to aging at 177 °C. The peak hardness, reached after 13 hours, was considerably lower than in the T6 temper, while the corresponding micrograph given in Figure 9(b) showed extremely coarse β'' precipitates having a median length of 64 nm (Figure 10(b)). Such a coarse microstructure, observed in both specimens, is characteristic of alloys containing higher levels of Mg and Si, such as 6061, which have been exposed to reduced temperature prior to artificial aging, and results in reduced tensile properties.^[28]

These results clearly show that aging at 65 °C only, prior to artificial aging, does not refine or increase the density of the precipitates in the microstructure of 6061, while exposure to RT prior to artificial aging has a strongly detrimental effect on both the microstructure and the hardness of 6061. The DSC scans were performed in order to explain this behavior. Figure 11 shows the DSC scans obtained from 6061 specimens aged for 2 weeks at 25 °C and at 65 °C, as well as from the material aged at 177 °C only for 5 and 20 minutes (the underaging stage of the T6I6 temper). These scans are compared to the scan from the as-solution-treated and quenched material.

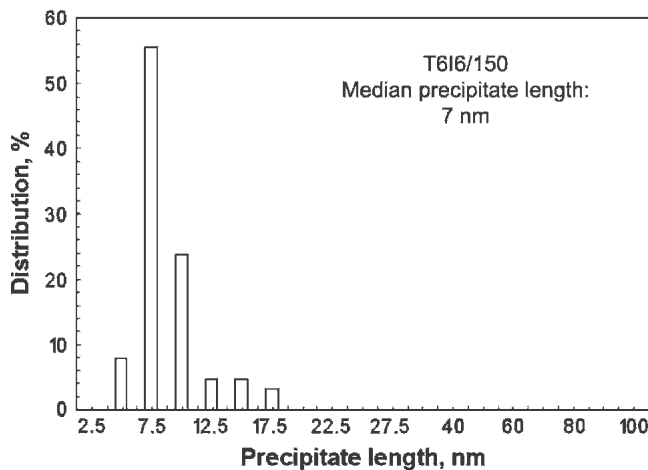
The scan from the as-solution-treated and quenched material shows four characteristic exothermic reactions consistent with results reported previously.^[11,12] Peak 1 corresponds to clustering of solute Mg and Si atoms; peak 2 indicates the formation of GP zones and appears as a shoulder of peak 3, which is associated with the formation of β'' precipitates; and peak 4 indicates the formation of β' precipitates. The DSC trace for the sample naturally aged for 2 weeks prior to heating in the DSC cell suggests that a considerable amount of clustering had occurred during natural aging, as indicated by the reduced area under peak 1. An endothermic reaction was then observed at about 200 °C, suggesting that the solute clusters formed during natural aging then dissolved on heating, thereby suppressing subsequent formation of GP zones under peak 2. This in turn appeared to affect the development of β'' , most likely causing these precipitates to form more coarsely and in a reduced number. In the specimen aged at 65 °C for 2 weeks, peak 1 was barely visible, indicating that the clustering reaction had been almost completed. However, as for



(a)



(b)



(c)

Fig. 7—Distribution of sizes (lengths) of elongated (β'') precipitates in the peak-aged tempers: (a) T6, (b) T6I6/177, and (c) T6I6/150.

the naturally aged specimen, it seems that these clusters/co-clusters were not sufficiently stable upon further heating, as they dissolved, possibly only partially (compare with the endothermic reaction for the naturally aged specimen),

between about 190 °C and 235 °C. The HRTEM examination did not reveal the presence of any discernable precipitates in the microstructures of the naturally aged specimen or the specimen aged at 65 °C for 2 weeks (Figure 12). This indicates that the solute aggregates detected by DSC and responsible for the hardness increase at 65 °C were fully coherent with the matrix and had insufficient size to give rise to significant contrast in the TEM. It is therefore believed that these solute aggregates were Mg and Si clusters/co-clusters.

In contrast to the scans from the specimens aged at the low temperatures, no endothermic reaction associated with dissolution of the co/-clusters was evident in the scans from the specimens aged at 177 °C for 5 and 20 minutes. The scan from the specimen aged for 5 minutes indicates that the clustering reaction had been almost completed in this time (absence of peak 1) and that these co/clusters had then transformed into GP zones during the scan. These subsequently evolved into β'' , as indicated by the broadening of peak 2, and possibly by the overlap between peaks 2 and 3. The scan from the specimen aged for 20 minutes again showed an absence of peak 1, with a significant amount of the precipitation characteristic of peak 2 already having taken place. These DSC scans confirm that the endothermic reaction ascribed to dissolution of the low-temperature co/-clusters, and the resulting development during artificial aging at 177 °C of a coarse microstructure with reduced mechanical properties, is prevented by underaging at 177 °C (followed by quenching).

IV. DISCUSSION

A. Correlation between the Mechanical Properties and the Microstructure of the T6I6 Temper

The T6I4 hardness curves given in Figure 2 show that 6061 initially underaged at 177 °C and quenched continued to harden when left at 65 °C, even after achieving a hardness close to that in the peak-aged T6 condition. The shorter the underaging period, the greater the response to secondary aging. This clearly indicates that secondary precipitation takes place in the underaged T6 6061 when quenched and left to age at reduced temperature. This effect can be attributed to the greater supersaturation of solute, and, possibly, to the greater concentration of vacancies than for specimens underaged for longer times.

The alloy responded well to the T6I6 aging treatment with the hardness being increased by ~8 pct when compared to the T6 temper. A marked improvement in the 0.2 pct proof stress (8 pct higher than that of the T6 temper) was also achieved through the T6I6/177 heat treatment without an appreciable change in the ductility of the alloy. This is consistent with recent studies on other alloys by Lumley *et al.*^[1,2,3]

It is known that the strengthening of age-hardenable aluminum alloys depends strongly on the morphology, orientation, distribution, and size of the strengthening precipitates.^[24] Based on the BF TEM observations shown in Figure 4, the size, spacing, and number, as well as the relative ratio of precipitates having different morphologies, have all been modified by the T6I6 tempers. The TEM images in Figure 5 show that 20 minutes of underaging at

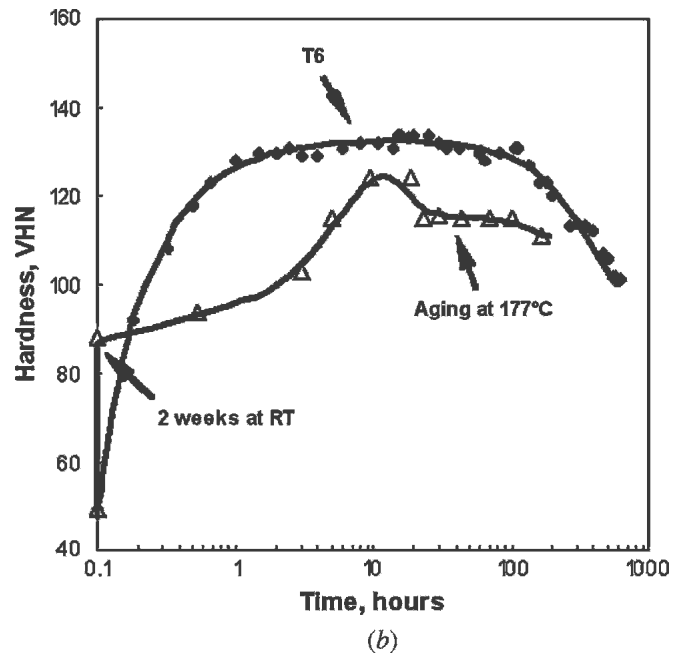
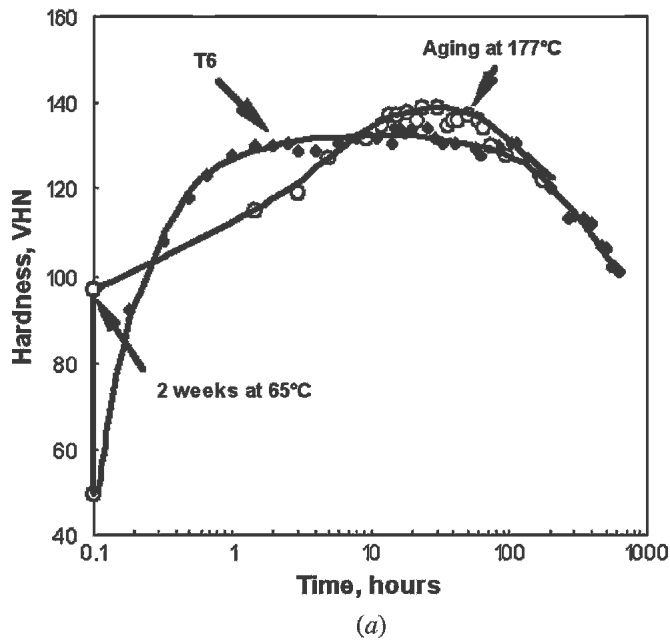


Fig. 8—Comparison of T6 age hardening curve (solid diamonds) with aging curve obtained from material (a) aged at 177 °C (open circles) following 2 weeks at 65 °C and (b) aged at 177 °C following 2 weeks at RT (open triangles).

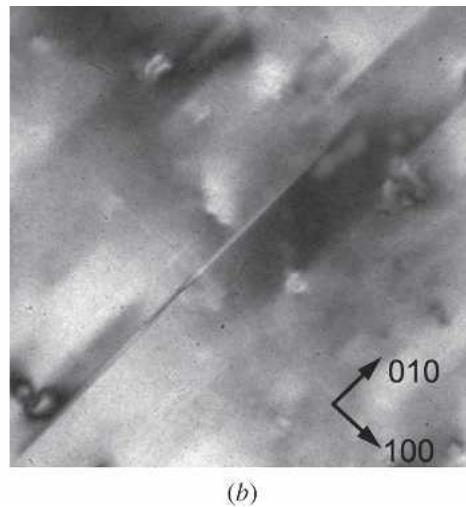
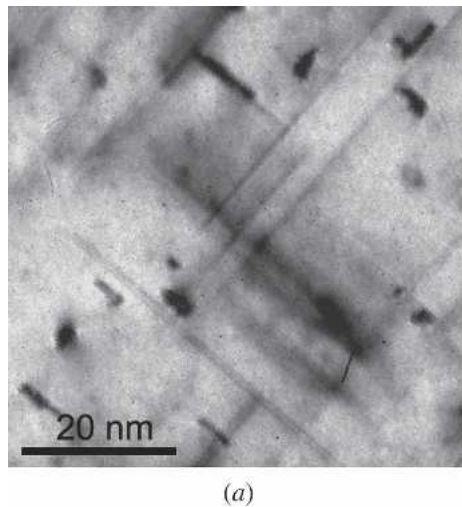
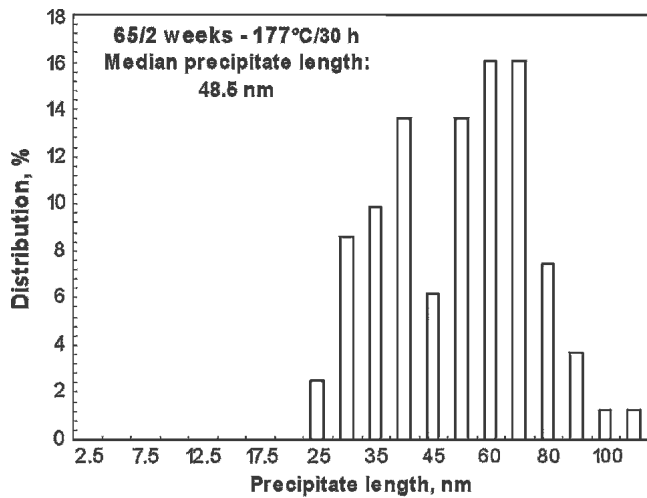


Fig. 9—BF TEM images showing peak-aged microstructures (a) after 30 h of aging at 177 °C following 2 weeks at 65 °C and (b) after 19 hours of aging at 177 °C following 2 weeks at RT.

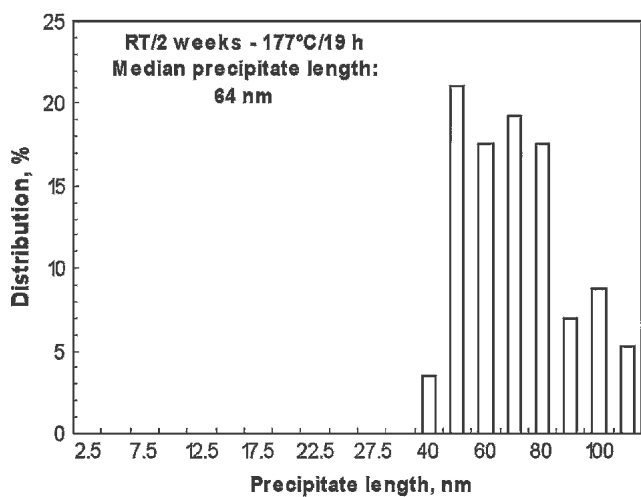
177 °C led to the precipitation of fully coherent GP zones, which would be expected to remain stable during aging at a lower temperature, such as 65 °C. After the interrupted aging stage at 65 °C, the density of the GP zones had increased substantially. This means that additional GP zones must have formed after a further 2 weeks at 65 °C, and, based on the TEM observations, these secondary GP zones attained a size similar to that of the GP zones already present, which is consistent with observations made elsewhere.^[5]

The GP zones are generally considered to be the precursors to the major strengthening phase (β'') in Al-Mg-Si-Cu alloys; thus, they would evolve into β'' precipitates during the reaging stage of the T6I6 heat treatments. It is plausible

that some GP zones formed late during the 65 °C dwell were below the critical size when heated to 177 °C or 150 °C and would therefore dissolve. Overall, however, the majority of the metastable GP zones appear to have remained in the microstructure and gradually evolved into β'' needles during the reaging stage of the T6I6 heat treatments. As a result, the β'' precipitates were more densely distributed, and therefore more closely spaced, following the T6I6 heat treatment than after a standard T6 temper. In addition, the T6I6 aging procedure decelerated the kinetics of precipitation and reduced the size of the precipitates. Well-defined β'' precipitates appeared later during reaging, while GP zones were observed even in the peak-aged T6I6 microstructures



(a)



(b)

Fig. 10—Distribution of sizes (length) of elongated (β'') precipitates in the peak-aged microstructures (a) after 30 h of aging at 177 °C following 2 weeks at 65 °C and (b) after 19 h of aging at 177 °C following 2 weeks at RT.

(Figure 4). This was ascribed to a great number of stable and concurrently evolving GP zones coupled with the reduced supersaturation of the solute in the matrix following the interrupted aging stage. As a result, the β'' needles in the peak-aged T6I6 tempers were much finer than in the peak-aged T6 temper.

The refined and modified microstructures resulting from the T6I6 tempers are considered to be directly responsible for the enhanced tensile properties. This was confirmed by more detailed comparison of the peak-aged microstructures of the T6, T6I6/177, and T6I6/150 tempers.^[25] The peak-aged microstructures of these three tempers all contained β'' as the dominant phase, but a considerable number of GP zones were also present. Although both GP zones and β'' contribute to age hardening, it is the partially coherent, needle-shaped β'' precipitates that are considered to be more effective obstacles to gliding dislocations than the fully coherent, and generally spherical, GP zones.^[26] The DF TEM images in Figure 6 indicated that the T6I6 heat

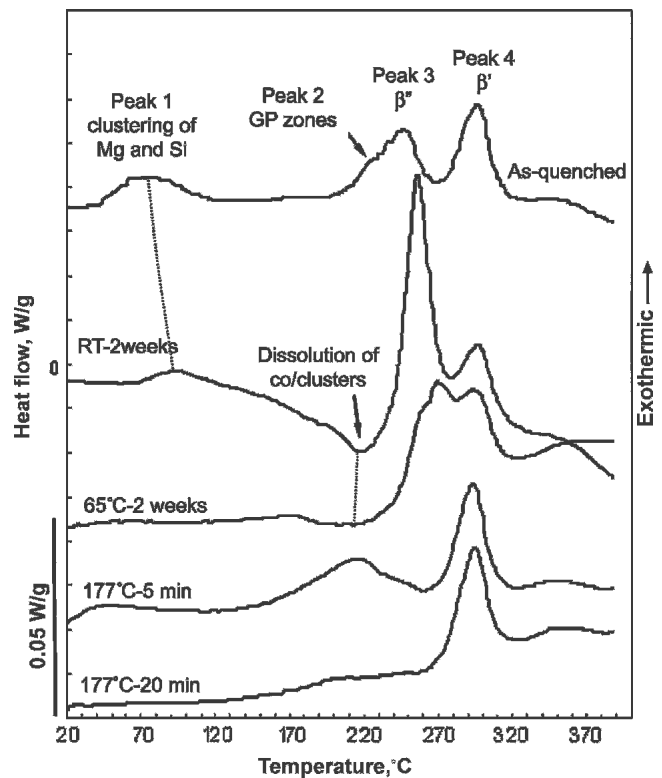


Fig. 11—DSC scans performed at a scan rate of 10 °C/min after solution treatment and quenching and aging at RT for 2 weeks, aging at 65 °C for 2 weeks, and aging at 177 °C for 5 and 20 min. The curves have been offset for clarity. The scan from the as-quenched specimen is given for comparison.

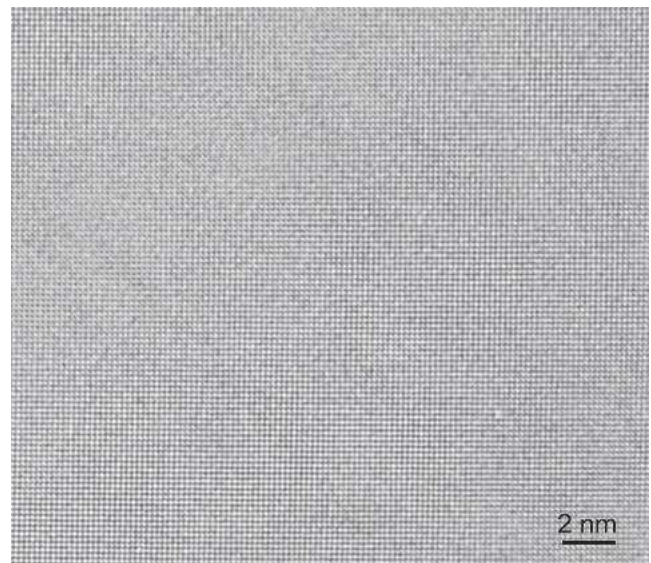


Fig. 12— $\langle 001 \rangle_\alpha$ HRTEM image of the specimen aged at 65 °C for 2 weeks.

treatment had indeed increased the density of the major strengthening phase, β'' , as part of the overall increase in the density of all precipitates in the peak-aged T6I6 microstructures. Furthermore, the results of the quantitative analysis shown in Figure 7(a) confirmed that the median length

of the β'' precipitates in the T6I6/177 temper (12 nm) was reduced to roughly one-third of the median length of the β'' in the T6 temper (35 nm). The presence of the fine β'' needles in the T6I6/177 temper, coupled with their increased density (and hence decreased spacing), was beneficial to the tensile properties of the material.

Less overall strengthening was achieved for the peak-aged T6I6/150 temper, although the density of precipitates appeared to be greater than in either the T6 or the T6I6/177 temper. In this case, the precipitates were substantially smaller than in the other two tempers. The ratio of fully developed β'' needles to very fine needles/GP zones was significantly lower than in the T6I6/177 and T6 microstructures. It is presumed therefore that, like GP zones, these underdeveloped and still coherent early forms of β'' provide only limited strengthening as they are easily cut by gliding dislocations.

The interrupted aging treatment also produced a substantial improvement in the fracture properties. The damage tolerance was increased by 21 pct in the T6I6/177 temper and by 36 pct in the T6I6/150 temper relative to that of the T6 temper. The simultaneous increase in tensile properties and damage tolerance of the alloy is unusual because these properties are commonly inversely related. However, similar results have been reported for other alloys by Lumley *et al.*^[1,2] A recent metallographic study of the fracture behavior in 6061 subjected to interrupted aging revealed that the T6I6 temper produced an increase in the average size of the microvoids generated during fracture.^[10] It was suggested that the modified size, spacing, and volume fraction of precipitate phases induced by interrupted aging may result in greater homogeneity of plastic flow during deformation and thereby delay, or impede, coalescence of microvoids, which is necessary for fracture.

B. Significance of High-Temperature Underaging

It is clear from Figures 4 and 5 that by promoting precipitation of the precursors (GP zones) to the major strengthening phase in Al-Mg-Si-Cu alloys (β''), subsequent aging led to the precipitation of a greater number of fine and densely distributed particles of β'' in the peak-aged condition. However, if the alloy is only preaged at 65 °C, or at RT prior to high-temperature artificial aging, the β'' precipitates that form are relatively large and coarsely dispersed at the peak hardness condition.

It has been reported that the precipitates that normally form at these low preaging temperatures are co/-clusters of Mg and Si.^[12,16,17] Although these very fine solute aggregates may induce considerable hardening, they cannot serve as nuclei that can evolve into GP zones (and then β''), because most are thermodynamically unstable (they dissolve) when subsequently artificially aged at 177 °C. Instead, only a reduced number of GP zones are nucleated following the dissolution of co/-clusters, resulting in the formation of a more limited number of coarser β'' precipitates (Figure 9). This behavior is in accord with the recognized fact that storage of many 6xxx series alloys at low temperatures, between quenching and artificial aging, causes a reduction in the mechanical properties.^[27,28,29] The preceding results highlight the importance of first underaging at elevated temperature, per the T6I6 aging procedure as in order to promote

the formation of GP zones that subsequently evolve into the β'' precipitates. An appropriate level of underaging at an elevated temperature is necessary in order to group solute atoms and, most likely, vacancies into stable formations that would undergo further controlled and gradual evolution during secondary aging at reduced temperature (the interrupted aging stage). Recent positron annihilation lifetime spectroscopy measurements on 6061,^[30] as well as similar experiments performed on Al-Cu-Mg^[31] and Al-Zn-Mg alloys,^[32] have all indicated that vacancies may be trapped inside precipitates formed at elevated temperatures. If, instead, most of these vacancies remained in supersaturation in the solid solution, as occurs after solution treatment and quenching or after insufficient preaging at elevated temperature, precipitation of fine coclusters would take place during aging at reduced temperatures, such as 65 °C or 25 °C.^[30] As discussed earlier, these fine co/-clusters would dissolve at the temperature of final aging and thus cause the alloy to not reach optimum mechanical properties.

V. CONCLUSIONS

An investigation has been made of the effects of the novel heat treatment, termed T6I6, on the microstructure and mechanical properties of the Al-Mg-Si-Cu alloy AA6061. This aging treatment involves interrupting the standard T6 temper at 177 °C by a dwell period (I) at a lower temperature (*e.g.*, 65 °C) before resuming aging at 177 °C, or the slightly lower temperature of 150 °C.

The T6I6 heat treatment causes an overall improvement in the mechanical properties of 6061 as compared to the conventional T6 temper. Peak hardness was increased by about 6 pct in the T6I6/150 temper. For the T6I6/177 temper, the peak hardness was increased by 9 pct and the 0.2 pct proof stress by 8 pct. Damage tolerance of the alloy was significantly improved by both T6I6 variants, the increases being 21 pct for the T6I6/177 temper and 36 pct for the T6I6/150 temper.

The TEM observations showed that the precipitates formed in the T6I6 peak-aged microstructures were finer, more densely distributed, more closely spaced, and present in greater numbers than they were following the T6 temper. This modification to the microstructure is consistent with the improved mechanical properties observed for the interrupted aged material.

Refinement of precipitates in the T6I6 tempers is associated with secondary precipitation of GP zones during interrupted aging, resulting in a greater number of these precipitates being present in the microstructure than is possible in a single-stage T6 heat treatment. The GP zones are known to be the precursors to nucleation of the main strengthening phase β'' , so that a greater density of the β'' precipitates forms when artificial aging is resumed.

An appropriate underaging treatment at elevated temperature is needed for the alloy 6061 to benefit from precipitation during interrupted aging at 65 °C. Preaging only at 65 °C results in the formation of very fine precipitates that are most likely co/-clusters of Mg and Si, which are not precursors to β'' . Such fine co/-clusters dissolve upon reaging at elevated temperature, resulting in a microstructure containing coarse β'' precipitates and exhibiting lower mechanical properties.

ACKNOWLEDGMENTS

This work was supported by a CSIRO Postgraduate scholarship. The authors thank Comalco for providing material, and Professor Ian Polmear for helpful comments and input.

REFERENCES

1. R.N. Lumley, I.J. Polmear, and A.J. Morton: Australian Patent AU766929, 2004.
2. R.N. Lumley, I.J. Polmear, and A.J. Morton: *Mater. Sci. Forum*, 2002, vols. 396–402, pp. 893–98.
3. R.N. Lumley, I.J. Polmear, and A.J. Morton: *Mater. Sci. Technol.*, 2005, vol. 29 (9), pp. 1025–32.
4. R.N. Lumley, I.J. Polmear, and A.J. Morton: International Patent Application PCT/AU02/00234, 2002.
5. R.N. Lumley, I.J. Polmear, and A.J. Morton: *Mater. Sci. Technol.*, 2003, vol. 19 (11), pp. 1483–90.
6. H. Löffler: *Structure and Development of Al-Zn Alloys*, Akademie Verlag, Berlin, 1995, pp. 250–66.
7. H. Löffler, I. Kovacs, and J. Lendvai: *J. Mater. Sci.*, 1983, vol. 18, pp. 2215–21.
8. M.J. Starink, A.J. Hobson, I. Sinclair, and P.J. Gregson: *Mater. Sci. Eng. A*, 2000, vol. 289, pp. 130–42.
9. R.N. Lumley, I.J. Polmear, and A.J. Morton: *Acta Mater.*, 2002, vol. 50, pp. 3597–608.
10. R.G. O'Donnell, R.N. Lumley, and I.J. Polmear: *Proc. 9th Int. Conf. on Aluminium Alloys*, Brisbane, Australia, 2004, pp. 975–80.
11. I. Dutta and S.M. Allen: *J. Mater. Sci. Lett.*, 1991, vol. 10, pp. 323–26.
12. G.A. Edwards, K. Stiller, G.L. Dunlop, and M.J. Couper: *Acta Mater.*, 1998, vol. 46, pp. 3898–3904.
13. D.E. Laughlin and W.F. Miao: *Automotive Alloys II*, TMS, Warrendale PA, 1998, pp. 63–79.
14. D.J. Chakrabarti, B.K. Cheong, and D.E. Laughlin: *Automotive Alloys II*, TMS, Warrendale, PA, 1998, pp. 27–44.
15. D.J. Chakrabarti and D.E. Laughlin: *Progr. Mater. Sci.*, 2004, vol. 49, pp. 389–410.
16. M. Murayama and K. Hono: *Acta Mater.*, 1999, vol. 47, pp. 1537–48.
17. M. Murayama, K. Hono, M. Saga, and M. Kikuchi: *Mater. Sci. Eng. A*, 1998, vol. 250, pp. 127–32.
18. M. Takeda, F. Ohkubo, and T. Shirai: *J. Mater. Sci.*, 1998, vol. 33, pp. 2385–90.
19. L. Zhen and S.B. Kang: *Mater. Sci. Technol.*, 1998, vol. 14, pp. 317–23.
20. C.D. Marioara, S.J. Andersen, J. Jansen, and H.W. Zandbergen: *Acta Mater.*, 2003, vol. 51, pp. 789–96.
21. S.D. Dumolt, D.E. Laughlin, and J.C. Williams: *Scripta Metall.*, 1984, vol. 18, pp. 1347–52.
22. K. Matsuda, Y. Uteani, T. Sato, and S. Ikeno: *Metall. Trans. A*, 2001, vol. 32, pp. 1293–99.
23. S.J. Andersen: *Metall. Trans. A*, 1995, vol. 26, pp. 1931–37.
24. J.W. Martin: *Precipitation Hardening*, 2nd ed., Butterworth-Heinemann, Oxford, United Kingdom, 1998, pp. 78–125.
25. J. Buha: Ph.D. Thesis, University of New South Wales, Sydney, 2005, <http://adt.caul.edu.au/>, pp. 234–76.
26. J.F. Nie, B.C. Muddle, and I.J. Polmear: *Mater. Sci. Forum*, 1996, vols. 217–222, pp. 1257–62.
27. D.W. Pashley, J.W. Rhodes, and A. Sendorek: *J. Inst. Met.*, 1966, vol. 94, pp. 41–47.
28. D.W. Pashley, M.H. Jacobs, and J.T. Vietz: *Phil. Mag.*, 1967, vol. 16, pp. 51–63.
29. I.J. Polmear: *Light Alloys: from Traditional Alloys to Nanocrystals*, 4th ed., Butterworth-Heinemann Publishers, Oxford, United Kingdom, 2006, p. 141.
30. J. Buha, P.R. Munroe, R.N. Lumley, A.G. Crosky, and A.J. Hill: *Proc. 9th Int. Conf. on Aluminium Alloys*, Brisbane, Australia, 2004, pp. 1028–33.
31. R. Ferragut, A. Somoza, A. Dupasquier, and I.J. Polmear: *Mater. Sci. Forum*, 2002, vols. 396–402, pp. 777–82.
32. C.E. Macchi, A. Somoza, A. Dupasquier, and I.J. Polmear: *Acta Mater.*, 2003, vol. 51, pp. 5151–58.